



# Low cost active devices to estimate and prevent off-road vehicle from rollover

D. Dieumet, B. Thuilot, R. Lenain, M. Berducat

## ► To cite this version:

D. Dieumet, B. Thuilot, R. Lenain, M. Berducat. Low cost active devices to estimate and prevent off-road vehicle from rollover. AXEMA-EurAgEng Conference "Intensive and environmentally friendly agriculture: an opportunity for innovation in machinery and systems", Feb 2017, Villepinte, France. hal-02607282

**HAL Id: hal-02607282**

**<https://hal.inrae.fr/hal-02607282>**

Submitted on 16 May 2020

**HAL** is a multi-disciplinary open access archive for the deposit and dissemination of scientific research documents, whether they are published or not. The documents may come from teaching and research institutions in France or abroad, or from public or private research centers.

L'archive ouverte pluridisciplinaire **HAL**, est destinée au dépôt et à la diffusion de documents scientifiques de niveau recherche, publiés ou non, émanant des établissements d'enseignement et de recherche français ou étrangers, des laboratoires publics ou privés.

# Low cost active devices to estimate and prevent off-road vehicle from rollover

Dieumet Denis<sup>3\*</sup>, Benoit Thuilot<sup>1,2</sup>, Roland Lenain<sup>3</sup>, Michel Berducat<sup>3</sup>

<sup>1</sup>Clermont Université, Université Blaise Pascal, Institut Pascal, BP 10448, 63000 Clermont-Ferrand, France

<sup>2</sup>CNRS, UMR 6602, Institut Pascal, 63177 Aubière, France

<sup>3</sup>Irstea, 9 avenue Blaise Pascal, 63172 Aubière, France

\* Corresponding author: dieumet.denis@irstea.fr

**Abstract**—This paper proposes to investigate the use of active devices, able to anticipate for hazardous situations, by using low cost sensors. In this approach, the risk of rollover is considered thanks to the Lateral Load Transfer (LLT) metric, able to characterize gradually the dynamic mass repartition on the vehicle, without using expensive cell forces. In order to account for variable conditions, an observer algorithm is used in order to adapt on-line the grip conditions thanks to a dynamical yaw model. Once adapted, this model supply the dynamic variable influencing the evolution of LLT. This metric can then be estimated thanks to a second partial dynamic model considering the roll plane. Thanks to the vehicle parameters (mass, elevation of centre of gravity), the risk of rollover may be accurately computed.

**Keywords:** Robotics in Agriculture, Hydraulic Actuators, Active Security Devices, Rollover, Dynamics, Grape Harvester.

## I. INTRODUCTION

Nowadays, mobile robotics perfectly fits in the notion of technological progress, either for intervening in extension or instead of humans by releasing them of repetitive, laborious or dangerous activities. Areas benefiting from the growth of robotics are legion, notably in the field of agriculture. Indeed, thanks to a certain repeatability that they can bring in the work, mobile robots represent a coherent answer to the current bets of the agricultural sector (increased acreages cultivated, quality, productivity, yielding, etc.). However, because of the continued increase in the size and the speed motion of agricultural machinery [1] combined to variable and bad grid conditions associated to a large diversity of terrains, driving vehicles in off-road environment remains a dangerous and harsh activity. Driving difficulties may be also encountered when considering huge machines with possible reconfiguration of their mechanical properties (changes in mass and centre of gravity height for instance). As a consequence, for the sole agriculture sector, several fatal injuries are reported per year in particular due to rollover situations [2], [3], [4], [5].

In order to reduce accident consequences, passive protections such as Rollover Protective Structures - ROPS [6] or Slope Correction Systems are installed on tractors. However, protection capabilities of these structures are very limited [7] and the ROPS cannot be embedded on bigger machines due to mechanical design limitations.

Therefore, active safety devices allowing either to warn the operator or to act directly on vehicle control variables are promising solutions to reduce risks and avoid hazardous

situations. Nevertheless, if driving assistance systems (such as ESP [8] or ABS [9]) have been deeply studied for on-road vehicles and successfully improve safety, development of control stability systems dedicated to off-road vehicles is still being in its infancy [10], [11], [12].

Besides reducing the accident statistics in the agriculture field, the economic benefits of these systems would be also very important provided such new solutions are at a reasonable cost for the purchaser [13]. Thus, given the limited number of sensors required to evaluate the Lateral Load Transfer (hereafter denoted LLT), its physical meaning and its relative computational simplicity, this metric has been here chosen as a relevant stability criterion among several rollover indicators described in the literature [14].

This paper presents a control stability system to assess and avoid rollover risk in reconfigurable agricultural vehicles. In such platforms, stability assessment needs to be robust to intrinsic property changes such as vehicle load and elevation of center of gravity. Therefore, in Section IV, relying on a sensitivity based steepest descent algorithm, the estimated LLT in Section III and its intermittent measurement in Section II are coupled in order to adapt the vehicle parameters. Thereby, the estimated LLT supplies relevant values when the measured one is unavailable and allows then to monitor the stability of the vehicle whatever the state of the slope correction system, the soil type and the load of the machine. In Section V, the efficiency and the capabilities of the proposed algorithm are investigated through full scale experiments on an hazardous field by using a grape harvester equipped with exteroceptive and proprioceptive sensors. The experimental vehicle considered in this paper (a grape harvester) can be geometrically reconfigured according to terrain slope and mass changes as the grape receptacle is progressively filled.

## II. VEHICLE ROLLOVER PROPENSITY MEASUREMENT

### A. Rollover Metric Formulation and Interpretation

The Lateral Load Transfer is a stability metric based on the distribution of the normal wheel-terrain contact forces, that indicates nearness to wheel lift-off. More precisely, it is defined as the difference in normal forces on the left and right sides of the vehicle ([15], [16], see also Figure 1) and normalized with the overall normal contact forces.

$$LLT = \frac{F_{n1} - F_{n2}}{F_{n1} + F_{n2}} \quad (1)$$

The LLT range of variation is comprised in  $[-1 \ 1]$ , the extreme values meaning that the wheels of one side of the vehicle lift off. In practice, it is considered that the rollover is imminent when  $|LLT|$  reaches 0.8, i.e., 80% of the sprung mass is then distributed on one side of the vehicle. For

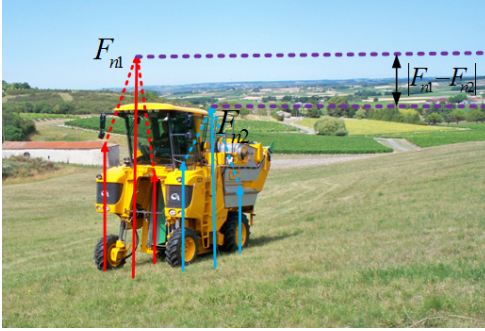


Fig. 1. Representation of the lateral load transfer

convenience purpose, hereafter the measured value and the estimated one will be denoted respectively  $\overline{LLT}$  and  $\widehat{LLT}$ .

### B. Rollover metric measurement

The hydraulic cylinders of the harvester used for slope correction are equipped with pressure sensors in order to enable force control. It is here proposed to use these sensors to obtain an indirect measurement of the actual LLT. More precisely, the pressure sensors located at the inlet and outlet chambers of the hydraulic actuators enable to measure the differential pressure in each cylinder connecting each axle to the suspended mass. Let us denote  $P_{ij}$  the differential pressure in the cylinder, where  $ij$  denotes the wheel,  $rr$  for right rear wheel for instance. The normal forces at the surface of contact of each wheel can be inferred from the differential pressure measurement in the cylinders as follows:

- The normal forces are  $K_{lf}P_{lf}$  and  $K_{rf}P_{rf}$  for respectively left and right front wheels,
- They are  $K_{lr}P_{lr}$  and  $K_{rr}P_{rr}$  for respectively left and right rear wheels

where  $K_{ij}$  are constant parameters that can be inferred from the diameter and the orientation of the cylinders. Since the rear (respectively the front) cylinders have the same diameter and a symmetric orientation, then  $K_{lr} = K_{rr} = \chi K_{lf} = \chi K_{rf}$  (where  $\chi$  is a constant) and in view of (1) the actual LLT value is eventually available from the pressure measurements according to:

$$\overline{LLT} = \frac{P_{lf} - P_{rf} + \chi(P_{lr} - P_{rr})}{P_{lf} + P_{rf} + \chi(P_{lr} + P_{rr})} \quad (2)$$

Nonetheless, this measurement of wheels-ground contact forces obtained by exploiting the actuators state is not permanently available. Indeed, when actuators are in end stops or in slope correction, pressures are not representative of the suspension forces. As a result, in order to monitor the degree of stability of the vehicle whatever the state of the slope correction system, in the next section, we will develop an observer to estimate permanently the vehicle rollover risk in real time.

## III. ROLLOVER METRIC ESTIMATION

### A. Dynamics Vehicle model

It appears that the use of a complete 3D dynamic model may be hardly tractable and time consuming from an observation point of view [17] and with a low cost perception system. Hence, in order to allow control law developments, a multi-model approach, where the vehicle dynamics is split into two 2D frames, see Fig. 2, has been preferred.

In the yaw projection, the vehicle is considered as a bicycle (each axle is viewed as a wheel) and its motion is described perpendicularly to a plane defined by the wheel/ground contact points. The influence of the vehicle inclination is accounted via the addition of a component of the gravity force  $P_y = mg \sin \alpha$ . The velocity  $v$  of the rear axle and the steering angle  $\delta_F$  are the variables controlled by the driver. The other parameters and variables are:

- $L_F$  and  $L_R$  are respectively the front and rear vehicle half-wheelbases,
- $\psi$  is the vehicle yaw angle,
- $u$  is the linear velocity at the roll center  $O'$ ,
- $\beta$  is the global sideslip angle.

In the roll frame, the vehicle is viewed as a 2D system whose mass is suspended. In order to account for damping and stiffness, a restoring force  $F_a$  depending on the roll angle  $\varphi$  and the roll rate ( $\dot{\varphi}$ ) of the sprung mass is introduced as:

$$\vec{F}_a = \frac{k_r \varphi + b_r \dot{\varphi}}{h} \vec{y}_2 \quad (3)$$

where  $h$  is the distance between the roll center  $O'$  and the vehicle center of gravity  $G$ . The roll damping  $b_r$  and stiffness coefficient  $k_r$  are obtained thanks to a preliminary calibration using weight measurements at each wheel in different conditions. In addition, the following variables are used:

- $c$  is the vehicle track,
- $\alpha$  is the bank angle of the terrain,
- $\gamma = \varphi + \alpha$  is the overall bank angle in the roll frame,
- $I_x$ ,  $I_y$  and  $I_z$  are respectively the roll, pitch and yaw moments of inertia,
- $P = mg$  is the gravity force attached to the suspended mass in the roll projection (where  $g$  is the gravitational constant),
- $F_{n1}$  and  $F_{n2}$  are the normal components of the wheel/ground contact forces at the vehicle left and right sides.

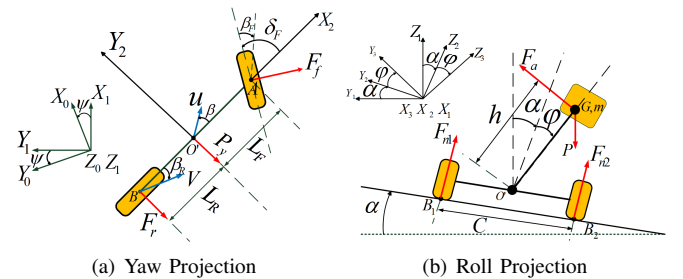


Fig. 2. Vehicle modeling into two frames

### B. Wheel/Ground interaction model

As illustrated in Figure 2(a), lateral contact forces at each wheel  $F_f$  and  $F_r$  are solely considered since this paper is only interested in the lateral risk of rollover. In order to avoid the use of complex tire/soil interaction models such as [18], these forces are assumed to be in linear relation with corresponding sideslip angles  $\beta_F$  and  $\beta_R$ , such as:

$$\begin{cases} F_f = C_f \beta_F \\ F_r = C_r \beta_R \end{cases} \quad (4)$$

with  $C_f, C_r > 0$ , cornering stiffnesses for the front and the rear axle. However, in order to account for the non-linear behavior of the tire and grip conditions variations, the cornering stiffnesses are adapted online relying on the backstepping observer proposed in previous work [19] and recalled below.

### C. Observer for grip conditions reconstruction via the Yaw model

The lateral dynamics observer is based on both the linear tire model (4) and the yaw model depicted in Fig. 2(a) and its general scheme is shown in Fig. 3. As detailed in

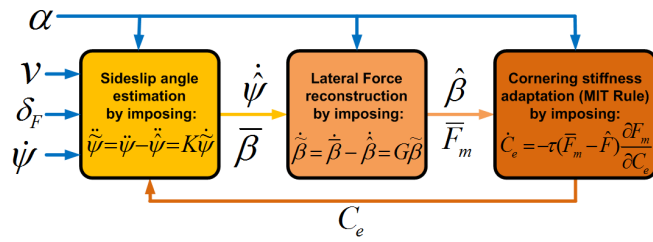


Fig. 3. Observer overview

Section V-A, the yaw rate ( $\dot{\psi}$ ), the rear axle linear velocity ( $v$ ) and the steering angle ( $\delta_F$ ) are measured. The terrain inclination ( $\alpha$ ) is estimated thanks to the measured lateral acceleration of the vehicle. These only four variables do not permit to estimate  $C_f$  and  $C_r$  separately. Thus, for observability reasons, they are supposed to be equal to a global virtual cornering stiffness  $C_e$ , i.e.,  $C_f = C_r = C_e$ . The backstepping observer is divided into three parts:

- The first one consists in computing a virtual measurement of the global sideslip angle (noted  $\hat{\beta}$  in Fig. 3). More precisely,  $\hat{\beta}$  is derived by imposing the convergence of the estimated yaw rate  $\hat{\psi}$  to the measured one  $\psi$ . This virtual global sideslip angle  $\hat{\beta}$  is then treated as a reference to be reached by the observed angle  $\hat{\beta}$ .
- In the second step, lateral contact forces are reconstructed by treating the global lateral contact force  $F_m = C_e(\beta_F + \beta_R)$  as a control variable (denoted  $\bar{F}_m$  in Fig. 3). More precisely,  $\bar{F}_m$  is obtained by imposing an exponential convergence on the observation error of the global sideslip angle  $\hat{\beta} = \hat{\beta} - \beta$ . Thereafter,  $\bar{F}_m$  is treated as reference to be reached by the observed one  $\hat{F}$ .

- Finally, since  $C_e$  is a slow varying parameter of force model (4), it has been obtained by imposing the convergence of the estimated force  $\hat{F}$  to  $\bar{F}_m$  by using the MIT rule adaptation law as presented in [20].

As mentioned in previous work [19], the observer is stable and ensures asymptotic convergence except when the vehicle is at stop ( $v = 0$ ), which is not considered here because at ( $v = 0$ ) there is no risk of rollover or when  $L_R = L_F$  which is never met on commercial tractors [21].

### D. Rollover Metric Estimation via the Roll Model

As detailed in [14], the fundamental principle of dynamics applied on the roll model depicted in Fig. 2(b) yields motion equations (6) in the roll frame. From the first equation of the roll model (6), the roll angle value ( $\varphi$ ) is derived and thereafter, the rollover risk (1) is estimated thanks to the two last equations of system (6). Figure 4 summarizes the process of *LLT* estimation relying on the partial dynamic approach used for modeling the vehicle. Indeed, thanks to the observer described previously, all the variables of the roll model are known, so that the *LLT* can be estimated from (1) and (6).

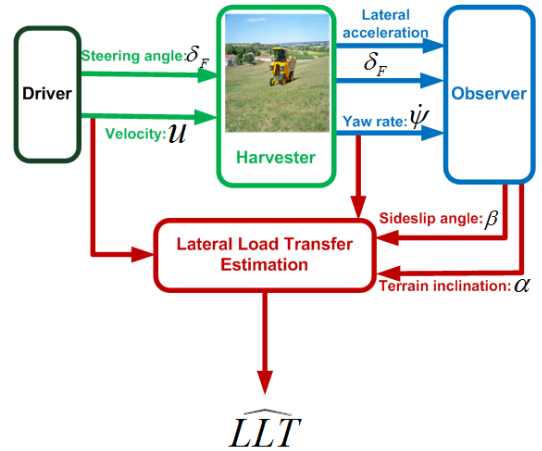


Fig. 4. Lateral Load Transfer Estimation Scheme

## IV. PARAMETRIC ADAPTATION FOR THE RELEVANCE OF THE ESTIMATED $\widehat{LLT}$

As pointed out before, the *LLT* estimation proposed in Section III requires the knowledge of several parameters that may be varying, such as the mass and the elevation of the center of gravity. Some off-road machines such as the experimental vehicle considered here, i.e., a grape harvester, can be geometrically reconfigured according to the terrain slope and its heaviness changes gradually when the grape receptacle is filled. Indeed, its heaviness may change in real time as the grape receptacle is progressively filling for instance. As a result, the estimated *LLT* may diverge from its actual value.

Hence, the aim of this section is to combine, when it is available, the discontinuous measurement of the *LLT* detailed in Section II with its estimation presented in Section III-D in order to update the vehicle varying parameters so that

the estimation algorithm can always deliver relevant  $\widehat{LLT}$  values. This then enables to monitor the stability of the vehicle whatever the state of the slope correction system, the soil type and the load of the machine.

#### A. Comparison and Coupling of measured and estimated Lateral Load Transfer

The idea is to update the height  $h$  and/or the mass  $m$  in order to ensure the convergence to zero of the error  $e$  between the measured and the estimated LLT. The general scheme is shown in Fig.5. More precisely, at each instant, the procedure is as follows:

- 1) Lateral Load Transfer measurement, according to equation (2),
- 2) If it is available,
  - Computation of the derivative of the height (respectively of the mass) according to equation (5) in order to ensure the convergence of the error  $e$  to 0,
  - Update of the height parameter (respectively of the mass) as:  $h = h + \dot{h}dt$  (respectively,  $m = m + \dot{m}dt$ ) where  $dt$  is the sampling period,
- 3) If  $\widehat{LLT}$  measurement is not available, then  $h$  and  $m$  remain unchanged.

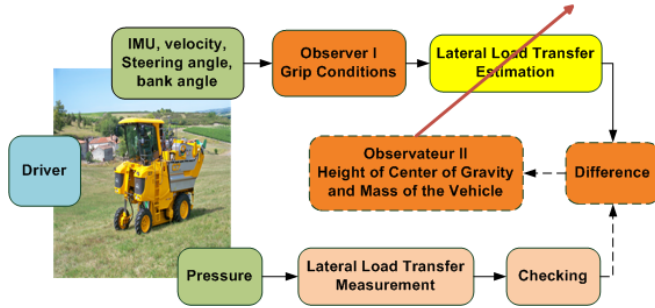


Fig. 5. Synopsis of the Estimator herein proposed

#### B. Adaptation of the vehicle suspended mass and of the height of the center of gravity

Provided that  $h$  and  $m$  are slow-varying parameters, which is a relevant assumption in the considered application, they can be adapted on-line, relying on a sensitivity based gradient search algorithm, in order for  $e = \widehat{LLT} - \overline{LLT}$  converges to 0. Then  $h$  and  $m$  should be adapted according to equations (5).

$$\begin{cases} \dot{h} = -\tau_1(.) e \frac{\partial \widehat{LLT}}{\partial h} \\ \dot{m} = -\tau_2(.) e \frac{\partial \widehat{LLT}}{\partial m} \end{cases} \quad (5)$$

where  $\tau_1(.) > 0$  and  $\tau_2(.) > 0$  are two varying gains controlling the dynamics of the convergence of the adapted parameters.

As it can be seen in the roll model (6),  $h$  and  $m$  have a similar influence on the estimated  $LLT$ . Nevertheless, mechanical constraints limit their evolution. Hence, in order

to compel the adapted values of the parameters to stay within their physical limits,  $\tau_1(.)$  and  $\tau_2(.)$  are designed as two sigmoid functions. Indeed, as depicted in Figure 6,  $\tau_1(.)$  is zero when  $h$  reaches its extreme values.  $\tau_2(.)$  is similarly defined. In the sequel, the height of the center of gravity is more likely to vary, for instance when the driver uses the slope correction system. Conversely, the vehicle weight is very slow varying parameter when the grape receptacle is being filled. Consequently,  $\tau_2(.)$  has been designed so that the adaptation of the height has a higher priority than the adaptation of the mass.

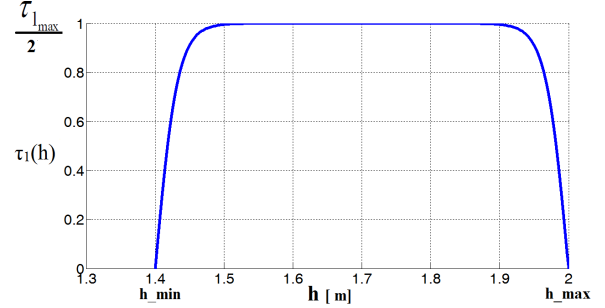


Fig. 6. Varying gain function of the height

## V. EXPERIMENTAL RESULTS

In order to highlight the efficiency of the proposed approach, some results obtained with a grape harvester are presented and discussed below.

#### A. Experimental vehicle and on boarded sensors

The experimental vehicle used to validate the proposed algorithm is a grape harvester manufactured by Gregoire SAS, depicted in Figure 1. As it can be seen, it is equipped with slope correction systems. The maximal inclination that can be imposed by this device is  $16.5^\circ$ . The total machine weight and the height of the center of gravity can vary during work respectively from 9 tons to 12 tons and from 1.4 m to 2 m and the maximal speed is 2 m/s.

The main sensors on-board, to be used by the algorithms described in this paper, are:

- a low cost IMU (Xsens), providing accelerations and angular velocities in three dimensions. Thanks to the lateral acceleration, the vehicle inclination ( $\alpha$ ) can also be known,
- a Doppler radar, supplying the vehicle velocity ( $v$ ) at the center of the rear axle,
- an angular sensor providing the steering angle  $\delta_F$ ,
- pressure sensors located at the inlet and outlet chambers of the hydraulic actuators, providing the differential pressures.

#### B. Validation of the proposed algorithm

The conditions of the test carried out to demonstrate the capabilities of the proposed algorithm are listed in Table I. The grape harvester moves on a sloping field (around  $10^\circ$ ), perpendicularly to the slope. As shown in Figure 7, the



$$\begin{cases} \ddot{\gamma} &= \frac{1}{h \cos \varphi} (h \dot{\gamma}^2 \sin \varphi + h \dot{\psi}^2 \sin \gamma \cos \alpha + u \dot{\psi} \cos \beta \cos \alpha + \dot{u} \sin \beta + u \dot{\beta} \cos \beta - \frac{F_a}{m} \cos \varphi + g \sin \alpha) \\ F_{n1} + F_{n2} &= m(-h \ddot{\gamma} \sin \varphi - h \dot{\gamma}^2 \cos \varphi + g \cos \alpha - \frac{F_a}{m} \sin \varphi - h \dot{\psi}^2 \sin \gamma \sin \alpha + u \dot{\alpha} \sin \beta - u \dot{\psi} \cos \beta \sin \alpha) \\ F_{n1} - F_{n2} &= \frac{2}{c} (I_x \ddot{\gamma} + (I_z - I_y) \dot{\psi}^2 \sin \gamma \cos \gamma - h \sin \varphi (F_{n1} + F_{n2})) \end{cases} \quad (6)$$

trajectory followed is composed of a straight line, a half turn and a straight line to go back to the starting point.

TABLE I  
TESTS CONDITIONS

<b>Vehicle load</b>	10.3 tons
<b>Velocity</b>	1.35 m/s
<b>Grip conditions</b>	Wet soil
<b>slope correction system</b>	On
<b>Height of the Center of Gravity</b>	1.7m

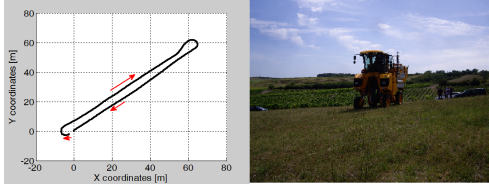


Fig. 7. Vehicle path

Figure 8(a) compares the estimated *LLT* (see Section III-D) and measured *LLT* (see Section II). The green graph was obtained by feeding the algorithm with the real values of the suspended mass and height of gravity, (i.e.,  $m = 10.3$  tons and  $h = 1.7$  m, see Table I). It can be noticed that the estimated *LLT* is properly superposed with the measured *LLT* (black graph) when this latter is available. This demonstrates the relevance of the estimation algorithm on difficult soil. The red graph was obtained when the estimation algorithm is fed with incorrect values for  $h$  and  $m$  and when these latter are not adapted (as it can be seen in Figures 8(c) and 8(d)). More precisely, the height ( $h = 1.4$  m) and the mass ( $m = 9$  tons) values are incorrects but they are realistic since they both belong to the admissible ranges (9 tons to 12 tons for  $m$ , 1.4 m to 2 m for  $h$ ). Fig. 8(a) shows in this case, the estimated *LLT* is not representative of the actual one and consequently could not be used to detect imminent rollover. This result demonstrates that the knowledge of the vehicle mass and height of the center of gravity is necessary for a relevant estimation of the *LLT*.

The graph in blue was obtained when initializing the estimation algorithm with the previous incorrect parameters values (i.e.,  $h = 1.4$  m and  $m = 9$  tons) but this time they were adapted on-line according to the gradient descent method (5). As soon as a measured *LLT* is available, the adaptation of the mass and of the height (see blue graphs in Fig. 8(d) and 8(c)) allows the estimated *LLT* to converge to its actual value. This demonstrates that the algorithm meets the expectations and allows to overcome the discontinuous availability of the *LLT* measure, even if  $h$  and  $m$  are poorly

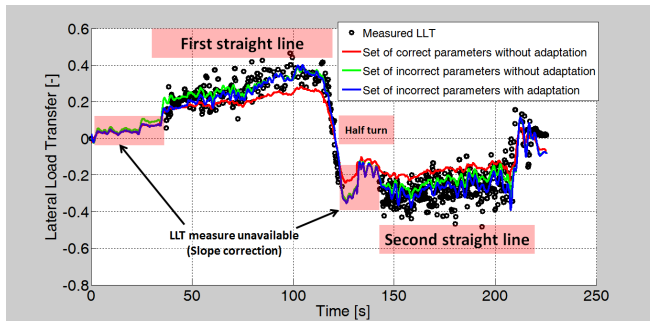
known.

As illustrated in Fig. 8(c), when the measure is not available (as a matter of fact between 124 and 141 seconds), the parameters adaptation is stopped as expected but the proposed algorithm continues to provide a reliable indicator of the risk of rollover. Indeed, when the *LLT* measure is again available at 141 seconds, i.e. just before the parameters are again adapted, the estimated *LLT* is still superposed with the measured one. This result demonstrates the algorithm robustness with respect to changes in vehicle geometry: as shown in Fig. 8(b) and 8(a), the driver used the slope correction system when he took the half-turn between 124 and 141 seconds. Thereafter, the overlap between the estimated and measured *LLT* is instantaneous. On many tests, it was found that the *LLT* measurement through the pressure sensors is often unavailable, showing the interest of the estimation presented in this paper.

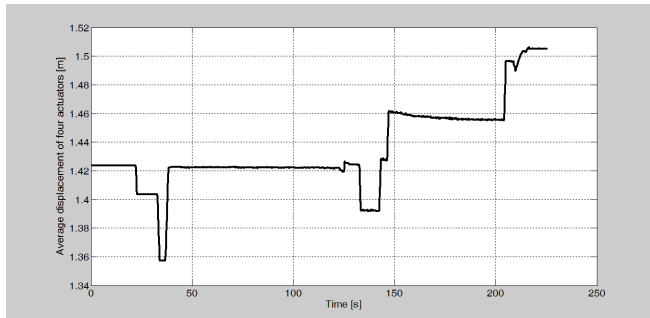
Finally, it is relevant to notice in Fig. 8(c) and 8(d), that the variation of  $h$  and  $m$  stays within their physical values. Indeed, the mass adaptation starts at 49 seconds, and 19 seconds later the real value of the mass is reached (i.e.,  $m = 10.3$  tons). Then, the adaptation of  $m$  is definitively stopped at its correct value. And without exceeding its correct value ( $h = 1.7$  m), the height adaptation continues to ensure the convergence of the estimated *LLT* to the measured one. As a result, the adaptive method described here can also be used as an indirect measurement of the variation of the vehicle mass which has an important interest in the agricultural field.

## VI. CONCLUSION AND FUTURE WORK

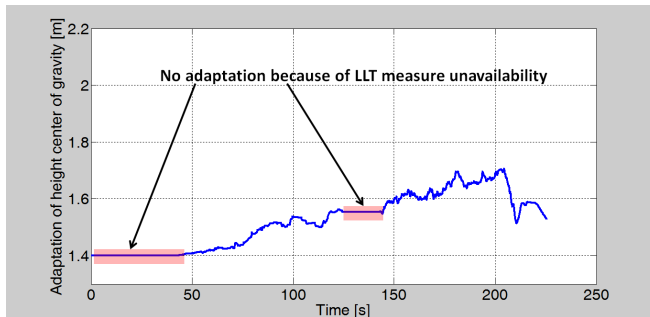
This paper has presented a control stability system based on-line estimation of the *LLT* metric continuously. Moreover, the latter can also be intermittently measured from the pressure sensors equipping the slope correction system of the grape harvester. The coupling of these discontinuous measurements with the estimated *LLT* allows the adaptation of vehicle parameters relying on a sensitivity based gradient search algorithm, so that the estimated *LLT* can always be relevant. This then allows to monitor the stability of the vehicle whatever the state of the slope correction system, the soil type and the load of the machine. As demonstrated in experiments, the multi-model approach chosen for modeling the vehicle is validated by the representativeness of the estimated *LLT* compared with the measured one. This online estimation method is implemented for the lateral load transfer evaluation, but it could also be applied similarly to evaluate the longitudinal load transfer. Hence, current work aims at extending the estimation method described here to the longitudinal risk of rollover. This work is also developed



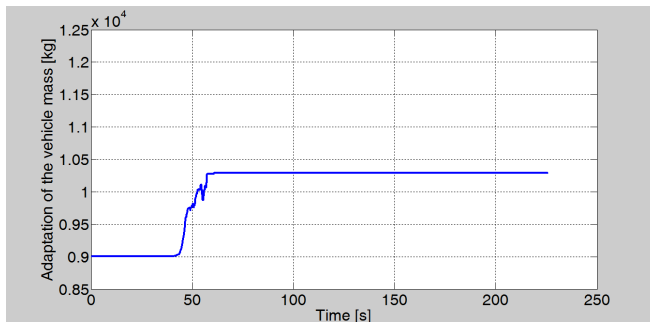
(a) Estimated and Measured Lateral Load Transfer



(b) Actuators displacement



(c) Height adaptation



(d) Mass adaptation

Fig. 8. Parameters adaptation for a relevant Lateral Load Transfer Estimation

further in order to anticipate the rollover risk by predicting the LLT values relying on the proposed vehicle models.

#### ACKNOWLEDGMENT

This work is supported by French National Research Agency (ANR) under the grant ANR-10-VPTT-008 at-

tributed to ActiSurTT project. It also received the support of French Agricultural Social Insurance (CCMSA) and French Ministry of Agriculture.

#### REFERENCES

- [1] S. Blackmore, B. Stout, M. Wang, and B. Runov, "Robotic agriculture - the future of agricultural mechanisation," *5th European Conference on Precision Agriculture (ECPA)*, Upsala (Sweden), 2005.
- [2] CCMSA, "Accidents du travail des salariés et non salariés agricoles," Observatoire des risques professionnels et du machinisme agricole, Paris, France, Tech. Rep., 2006.
- [3] M. Personick and J. Windau, "Self-employed individuals fatally injured at work," *United States Bureau of Labor Statistics*, Washington, DC, pp. 55–62, 1997.
- [4] N. S. Council, "Accident facts," National Safety Council, Chicago, IL, Tech. Rep., 1999.
- [5] J. M. Stellman, *Encyclopédie de santé et de sécurité au travail*. Bureau International du Travail, Genève, Suisse, 2000, vol. 4.
- [6] ASAE, "standards: roll-over protective structures (ROPS) for wheeled agricultural tractors (iso compatible)." *ASAE S519 DEC94*, 1997.
- [7] H. Cole, M. Myers, and S. Westneat, "Frequency and severity of injuries to operators during overturns of farm tractors," *Journal of Agricultural Safety and Health*, vol. 12, no. 2, pp. 127–138, 2006.
- [8] F. Tahami, R. Kazemi, and S. Farhanghi, "A novel driver assist stability system for all-wheel-drive electric vehicles," *IEEE Transactions on Vehicular Technology*, vol. 52, no. 3, pp. 683–692, 2003.
- [9] B. Guvenc, T. Bunte, and D. Odenthal, "Robust two degrees-of-freedom vehicle steering controller design," *IEEE Transactions on Control Systems Technology*, vol. 12, no. 4, pp. 627–636, 2004.
- [10] B. Paggi and M. Ribaldone, "Braking control system for agricultural tractors," *Same Deutz-Fahr: Italy*, 2000.
- [11] M. Kise and Q. Zhang, "Sensor-in-the-loop tractor stability control: Look-ahead attitude prediction and field tests," *Computers and Electronics in Agriculture*, vol. 52, no. 1-2, pp. 107–118, 2006.
- [12] J. Powers, J. Harris, J. Etherton, K. Snyder, M. Ronaghi, and B. Newbraugh, "Performance of an automatically deployable rops on asae tests," *Journal of Agricultural Safety and Health*, vol. 7, no. 1, pp. 51–61, 2001.
- [13] K. Owusu-Edusei Jr, "Net monetary benefit of cost-effective rollover protective structures (crops): An estimate of the potential benefits of the crops research project," *Journal of Agriculture Safety and Health*, vol. 14, no. 3, pp. 351–363, 2008.
- [14] D. Denis, "Contribution à la modélisation et à la commande de robots mobiles reconfigurables en milieu tout-terrain. application à la stabilité dynamique d'engins agricoles," Ph.D. dissertation, Université Blaise Pascal, Clermont-Ferrand II, 2015.
- [15] D. Odenthal, T. Bunte, and J. Ackerman, "Nonlinear steering and braking control for vehicle rollover avoidance," *Proc. of European Control Conference (ECC)*, Budapest (Hongrie), 1999.
- [16] B. Chen and H. Peng, "Differential-braking-based rollover prevention for sport utility with human-in-the-loop evaluations," *Vehicle System Dynamic*, pp. 359–389, 2001.
- [17] G. Genta, "Motor vehicle dynamics: Modeling and simulation," *World Scientific*, 1997.
- [18] H. Pacejka, *Tire and vehicle dynamics*. Society of Automotive Engineers, 2002.
- [19] M. Richier, R. Lenain, B. Thuilot, and C. Debain, "On-line estimation of a stability metric including grip conditions and slope: Application to rollover prevention for all-terrain vehicles," in *Proceedings of IEEE/RSJ International Conference on Intelligent Robots and Systems, IROS'11*, San Francisco, U.S.A, pp. 4569–4574, 25-30 Sept. 2011.
- [20] K. Åström and B. Wittenmark, "Adaptive control (2nd edition)," *New-York*, Addison-Wesley, 1994.
- [21] D. Denis, A. Nizard, B. Thuilot, and R. Lenain, "Slip and cornering stiffnesses observation for the stability assessment of off-road vehicles," in *Workshop "Transports, Mobility and Vehicles" at Mediterranean Green Energy Forum (MGEF)*, Marrakech (Morocco), 2015.